Iranian Journal of Oil & Gas Science and Technology, Vol. 7 (2018), No. 3, pp. 73-100
http://ijogst.put.ac.ir

Application of an Adaptive Neuro-fuzzy Inference System and Mathematical Rate of Penetration Models to Predicting Drilling Rate

Hossein Yavari[1], Mohammad Sabah[2*], Rassoul Khosravanian[3], and David A. Wood[4]

[1] M.S. Student of Petroleum Department of Amirkabir University of Technology, Tehran, Iran
[2] M.S. Student of Petroleum Department of Amirkabir University of Technology, Tehran, Iran
[3] Assistant Professor of Petroleum Department of Amirkabir University of Technology, Tehran, Iran
[4] DWA Energy Limited, Lincoln, United Kingdom

Received: April 27, 2017; *revised*: May 22, 2017; *accepted*: June 17, 2017

Abstract

The rate of penetration (ROP) is one of the vital parameters which directly affects the drilling time and costs. There are various parameters that influence the drilling rate; they include weight on bit, rotational speed, mud weight, bit type, formation type, and bit hydraulic. Several approaches, including mathematical models and artificial intelligence have been proposed to predict the rate of penetration. Previous research has showed that artificial intelligence such as neural network and adaptive neuro-fuzzy inference system are superior to conventional methods in the prediction of drilling rate. On the other hand, many complicated analytical ROP models have also been developed during recent years that are able to predict drilling rate with a high degree of accuracy. Therefore, comparing different approaches to find the most accurate model and assess the conditions in which each model works well can be highly effective in reducing drilling time as well as drilling cost. In this study, Hareland-Rampersad (HR) model, Bourgoyne and Young (BY) model, and an adaptive-neuro-fuzzy inference system (ANFIS) are employed to predict the drilling rate in the South Pars gas field (SP) offshore of Iran, and their results are compared to find the best ROP-prediction model for each formation. A database covering the drilling parameters, sonic log data, and modular dynamic test data collected from several drilling sites in SP are used to construct the mentioned models for each formation. The results show that when a large amount of data is available, the ANFIS is more accurate than the other approaches in predicting drilling rate. In the case of ROP models, BY model works considerably better than HR model for the majority of the formations. However, in formations where some drilling parameters are constant, but formation strength is variable, HR model shows better prediction performance than BY model.

Keywords: Rate of Penetration (ROP), ANFIS, Bourgoyne and Young, Hareland-Rampersad, Simulated Annealing Algorithm (SAA)

1. Introduction

The exploration and development of gas and oil fields require the efficient and cost-effective drilling of well bores, which can be achieved through the optimization of several variables (Aghajanpour et

* Corresponding Author:
Email: mohamadsabah@aut.ac.ir

al., 2017; Alexeyev et al., 2017; Eren, 2010a). The rate of penetration (ROP) is one of the important parameters, which should be predicted and optimized to reduce the drilling costs. There are various parameters which significantly affect the drilling rate, some of which include formation properties, weight on bit, bit rotational speed, bit type, hydraulic, and bit wear; these parameters make drilling rate render its behavior non-linear and difficult to predict.

Several researchers have investigated the effects of drilling parameters on the rate of penetration. Bilgesu et al. (1997) modeled the rate of penetration and bit wear using a new neural network under various formation types and drilling parameters. In their work, the operational parameters such as formation type, torque, weight on bit, rotational speed, and hydraulic horsepower are considered to predict drilling rate. Xiangchao Shi et al. (2015) employed a new confined compressive strength (CCS) model combined with specific mechanical energy to optimize the operational parameters. Their results showed that these parameters could be used to detect efficient drilling situations. Bodaghi et al. (2015) established a formulation between drilling variables and the rate of penetration by using optimized support vector regression. For this purpose, the genetic and cuckoo search algorithms were utilized to optimize the support vector regression. Following this, Ansari et al. (2016) predicted the rate of penetration by using a method based on imperialist competitive algorithm. Kahraman (2016) predicted the drilling rate by using artificial neural network and a multiple regression method. In addition to operational parameters, uniaxial compressive strength, tensile strength, and relative abrasiveness were considered as the input variables. Their results showed that the artificial neural network was more reliable than multiple regression method to predict the ROP. In a study of Khandelwal et al. (2016), multiple regression method, artificial neural network, and hybrid genetic algorithm were used to estimate the drilling rate. The comparison of the results showed that the hybrid genetic algorithm had better performance in ROP prediction compared to the other models. Yi et al. (2014) used a shuffled frog algorithm to obtain optimum values of drilling parameters. Weight on bit, bit rotational speed, flow rate, and bit tooth wear are some of the variables considered in their study. Jiang et al. (2016) combined an artificial neural network and ant colony optimization (ACO) to acquire optimum values for drilling rate. They considered the weight on bit, rotational speed, flow rate, and gamma ray as the input variables. Xian Shi et al. (2016) used an extreme learning machine, an upper-layer solution aware model, and an artificial neural network to predict drilling rate. Their results indicated that all of these methods can be an appropriate method to predict the drilling rate. Hegde et al. (2015) predicted the rate of penetration by using statistical learning techniques such as trees, bagged trees, and random forests; these techniques were used for a data set with nine predictors. Khosravanian et al. (2016) used the fuzzy inference systems (FIS) of Sugeno and Mamdani to predict the weight on bit. According to their results, Sugeno-type FIS is more accurate than Mamdani-type FIS in the prediction of weight on bit. Moraveji et al. (2016) investigated the effect of six variables on ROP. They used response surface methodology to develop a mathematical relation between drilling rate and drilling parameters such as depth, weight on bit (WOB), RPM, jet impact force, yield point to plastic viscosity ratio, and 10 min-to-10 s gel strength ratio. They used bat algorithm to optimize drilling parameters to reach the maximum ROP. Their results showed that this model provided an efficient tool for the prediction and optimization of drilling rate. Monazami et al. (2012) utilized ANN for the prediction of ROP in one of Iranian oil fields. Their results showed that ANN is a useful tool for the prediction of ROP, especially when the relationships between drilling parameters and ROP are too complicated.

Arabjamaloei et al. (2011) used ANN to predict the drilling rate in one of the Iranian oil fields, and they then optimized the drilling parameters using genetic algorithm to achieve the maximum drilling rate. There was good agreement between their results and the real field data, indicating that the ANN

was able to predict the drilling rate accurately. Basarir et al. (2014) compared the performance of linear regression, non-linear regression, and ANFIS for the prediction of ROP. Their results showed that ANFIS is the most accurate method compared to the regression methods. The previous researches proved that the ANN is able to predict the ROP and other parameters such as permeability, minimum miscibility pressure, and stuck pipe when a large data set is available (Afshari et al., 2014; Ahmadi et al., 2012, 2013; Arabjamaloei et al., 2011; Asoodeh et al., 2015; Monazami et al., 2012; Rabiei et al., 2015; Hedayat Rahimzadeh et al., 2010; Shadizadeh et al., 2010; Zoveidavianpoor et al., 2013b). Since ANFIS is a combination of artificial neural network and fuzzy logic (Zoveidavianpoor et al., 2013a), it is expected that its results are more accurate than ANN in cases which a low amount of data exists (Basarir et al., 2014). Therefore, in this study, based on the number of available data, ANFIS is utilized to predict ROP.

Clearly, several approaches have been employed to predict the drilling rate and to optimize the drilling parameters to various degrees of accuracy in recent years (Hedayat Rahimzadeh et al., 2010). It is worth noting that the accuracy of these approaches depends on various parameters such as drilling condition, drilling variables, and the number of data points they incorporate. Selecting the most accurate approach for predicting the drilling rate can be extremely beneficial to reducing the drilling time as well as drilling costs.

In this study, Hareland-Rampersad (HR) model and Bourgoyne and Young (BY) model, which are the most widely used ROP models, together with an adaptive-neuro-fuzzy-inference system (ANFIS) are used to predict the ROP in the South Pars (SP) gas field offshore of Iran. Their results are compared to find the most proper model for each formation and to assess the conditions in which each model works well.

2. Field information and data analysis

SP gas field consists of various phases, and the drilling data of one of these phases have been used in this study. Due to confidentiality purposes, the name of the field development phase and specific well numbers cannot be disclosed. The geological formations penetrated by the wells of the SP phase studied, in order of the shallowest to the deepest, consist of the Asmary, Ilam, Sarvak, Upper limestone, Dashtak, Surmeh, and Kangan.

All the information, which are required to construct ROP models for each formation, have been extracted from the daily mud logging reports (DMLR), modular dynamic test (MDT), and sonic log data. The extracted drilling data include drilling rate, weight on bit (WOB), rotational speed (RPM), pump flow rate, mud weight, bit type, and bit wear. Modular dynamic test and sonic log data are used to estimate the pore pressure and uniaxial compressive strength respectively. The overall data set consists of 721 records divided randomly into two parts, in which 70% (504 data records) of the overall data are used to construct (train) the model, and the remaining 30% (217 data records) are employed to test the developed model. All the data used herein are displayed graphically in Figures 1-2.

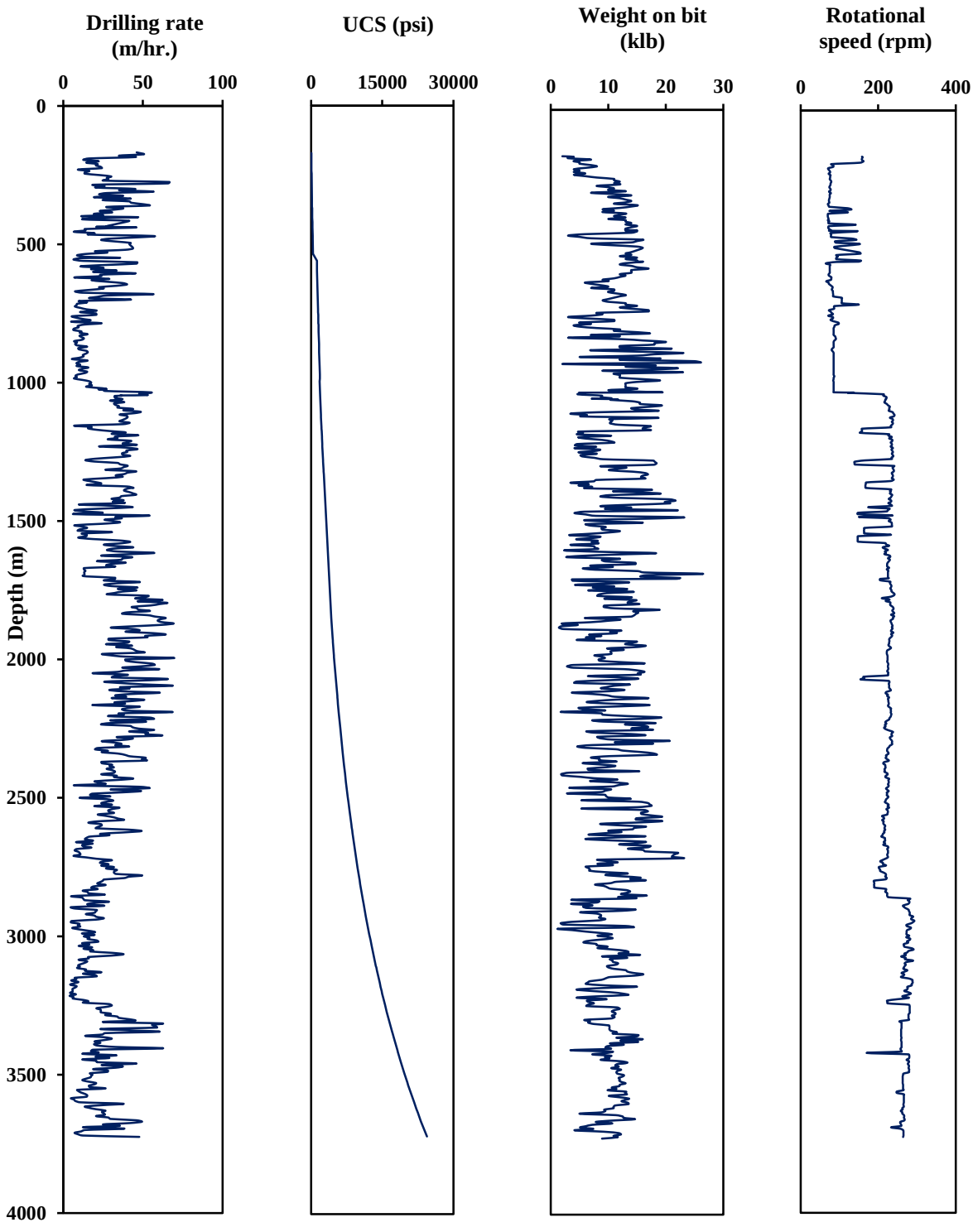

Figure 1
Drilling data extracted from daily drilling reports of one of the wells.

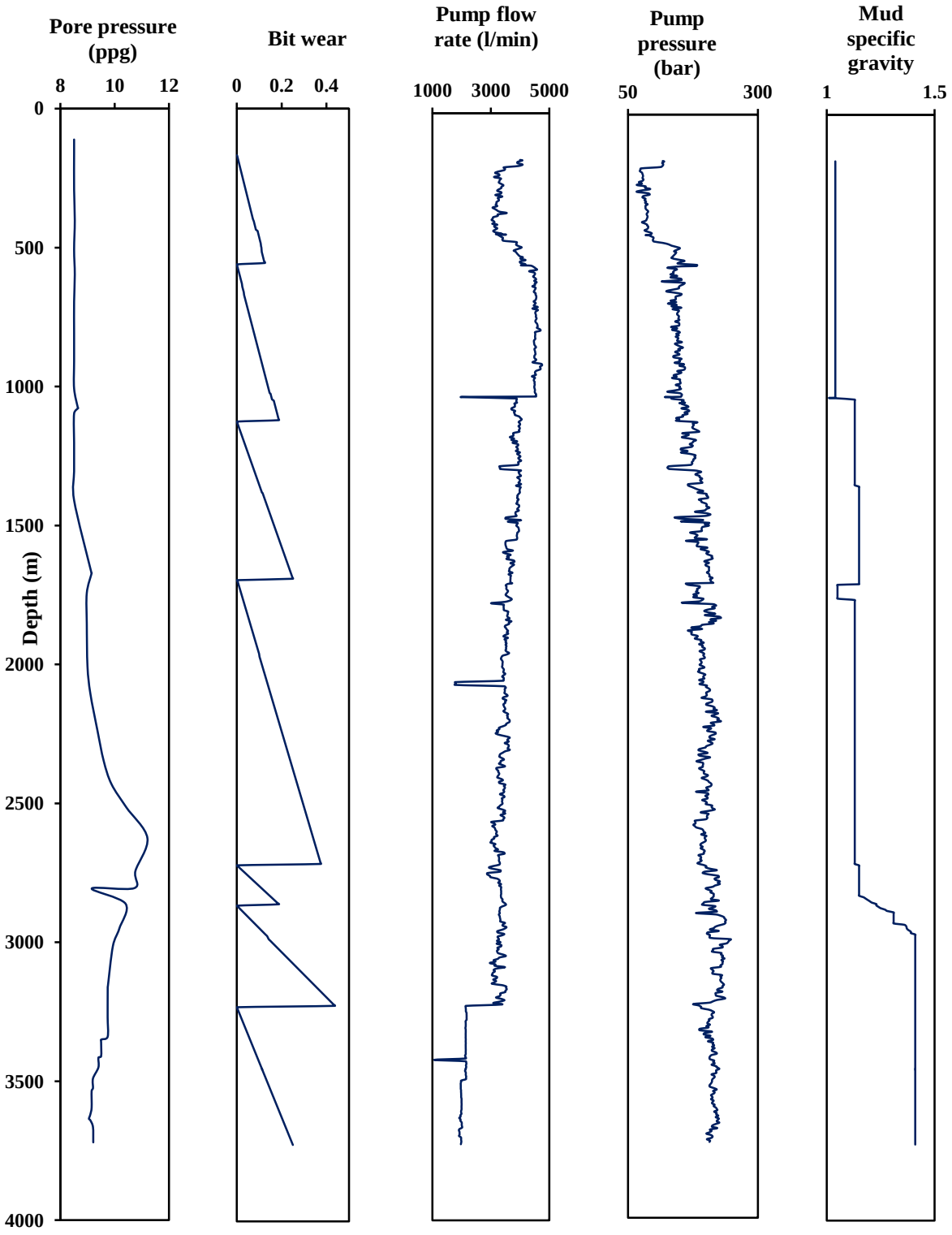

Figure 2
Drilling data extracted from daily drilling reports, pore pressure, and modular dynamic test data.

3. Bourgoyne and Young (BY) model

Several models have been suggested to predict the rate of penetration. The model established by Bourgoyne and Young (Bourgoyne Jr. et al., 1974) is one of the most complete drilling models used for roller cone bits (Nascimento et al., 2015). They suggested using eight functions to model the influence of different drilling parameters such as weight on bit, rotary speed, bit wear, formation strength, and jet impact force. Bourgoyne-Young drilling model is defined by Equation 1:

$$ROP = (f_1)(f_2)(f_3)(f_4)(f_5)(f_6)(f_7)(f_8) \tag{1}$$

where,

$$f_1 = e^{2.303a_1} \tag{2}$$

$$f_2 = e^{2.303a_2(10000-D)} \tag{3}$$

$$f_3 = e^{2.303a_3D^{0.69}(P_p-9)} \tag{4}$$

$$f_4 = e^{2.303a_4D(P_p-ECD)} \tag{5}$$

$$f_5 = \left[\frac{\frac{WOB}{d_b} - \left(\frac{WOB}{d_b}\right)_t}{4 - \left(\frac{WOB}{d_b}\right)_t}\right]^{a_5} \tag{6}$$

$$f_6 = \left[\frac{N}{60}\right]^{a_6} \tag{7}$$

$$f_7 = e^{-a_7h} \tag{8}$$

$$f_8 = \left[\frac{F_j}{1000}\right]^{a_8} \tag{9}$$

in which, D (ft.) is the true vertical-well depth, and P_p (lbm/gal) represents the pore-pressure gradient; ECD (lbm/gal) is the equivalent circulating density, and $\left(\frac{WOB}{d_b}\right)_t$ (1000 lbf/in) stands for the threshold bit weight per inch of bit diameter at which the bit begins to drill; h is the fractional tooth wear; F_j (lbf) denotes the hydraulic impact force beneath the bit, and a_1 through a_8 are the constants which must be chosen on the basis of local drilling conditions. All the information required to construct this model for each formation is extracted from daily mud logging reports (DMLR) and modular dynamic test (MDT) data. The multiple regression method is utilized to determine the model constants (a_1 through a_8) for each formation. Initially, Bourgoyne and Young model needs to be expressed in a linear form; the linear form is obtained by taking the natural logarithms of both sides of Equation 1. Equation 10 shows the linear form of the BY model. Table 1 lists the values of X_2 to X_8 in the linear form of Bourgoyne and Young model.

$$Y = Ln(ROP) = K_s + a_1X_1 + a_2X_2 + a_3X_3 + a_4X_4 + a_5X_5 + a_6X_6 + a_7X_7 \tag{10}$$

Table 1
Coefficients of linear form of Bourgoyne and Young model.

Characteristic	Variable	Amount
Normal compaction parameter	X_1	$2.303 *\times (10000 - D)$
Under compaction parameter	X_2	$2.303 \times D^{0.69} \times (g_p - 9)$
Pressure differential parameter	X_3	$2.303 \times D * (g_p - \rho)$
Bit weight parameter	X_4	$Ln\left(\frac{\left(\frac{W}{d}\right) - \left(\frac{W}{d}\right)_t}{4 - \left(\frac{W}{d}\right)_t}\right)$
Rotary speed parameter	X_5	$Ln\left(\frac{N}{60}\right)$
Tooth wear parameter	X_6	$-h$
Hydraulic parameter	X_7	$Ln\left(\frac{F_j}{1000}\right)$

The X and Y values (Equation 10) are then determined using the data set. The general form of multiple-linear regression (MLR) for a problem with k constants is as shown in Equation 11, where n is the number of the data records involved (Eren, 2010b). By solving this matrix, the constants can be determined:

$$\begin{bmatrix} \sum_{i=1}^{n} i & \sum_{i=1}^{n} X_{i1} & \sum_{i=1}^{n} X_{i2} & \cdots & \sum_{i=1}^{n} X_{ik} \\ \sum_{i=1}^{n} X_{i1} & \sum_{i=1}^{n} X_{i1}^2 & \sum_{i=1}^{n} X_{i1}X_{i2} & \cdots & \sum_{i=1}^{n} X_{i2}X_{ik} \\ \vdots & \vdots & \vdots & & \vdots \\ \sum_{i=1}^{n} X_{ik} & \sum_{i=1}^{n} X_{ik}X_{i1} & \sum_{i=1}^{n} X_{ik}X_{i2} & & \sum_{i=1}^{n} X_{ik}^2 \end{bmatrix} \begin{bmatrix} a_0 \\ a_1 \\ a_2 \\ a_3 \\ \vdots \\ a_k \end{bmatrix} = \begin{bmatrix} \sum_{i=1}^{n} y_i \\ \sum_{i=1}^{n} x_{i1}\, y_i \\ \sum_{i=1}^{n} x_{i2}\, y_i \\ \vdots \\ \sum_{i=1}^{n} x_{ik}\, y_i \end{bmatrix} \quad (11)$$

Multiple-linear regression is an accurate method for determining the constant coefficients of a model, but sometimes, because of the quality of the existing data (e.g. anomalous data points in certain data records), it leads to meaningless constants (e.g. calculating negative ROP's), especially when applied to Bourgoyne and Young model. In this situation, the abnormal data points need to be removed from the data set. In addition, there are some numerical methods for determining the constant coefficients. In this study, the simulated annealing algorithm was utilized to determine Bourgoyne and Young model constants when MLR leads to meaningless constants.

Simulated annealing algorithm

In 1983, Kirkpatrick et al. (1983) successfully used the simulation of physical annealing in optimization. The parameters of simulated annealing algorithm (SAA) include the design variables (X_0); the energy state ($E(X_0)$),which is equivalent to the objective function; the initial temperature (T_0); the freezing temperature (T_f); the length of Markov chain (L); and temperature decrement factor (α)

(Granville et al., 1994). SAA uses a Metropolis criterion to escape from local optimum point and to have a better chance to obtain the global optimum point. The acceptance probability of the Metropolis criterion is as follows (Metropolis et al., 1953).

$$P = exp\left(-\frac{\Delta E}{T}\right) \tag{12}$$

Figure 3 shows the flowchart of the simulated annealing algorithm.

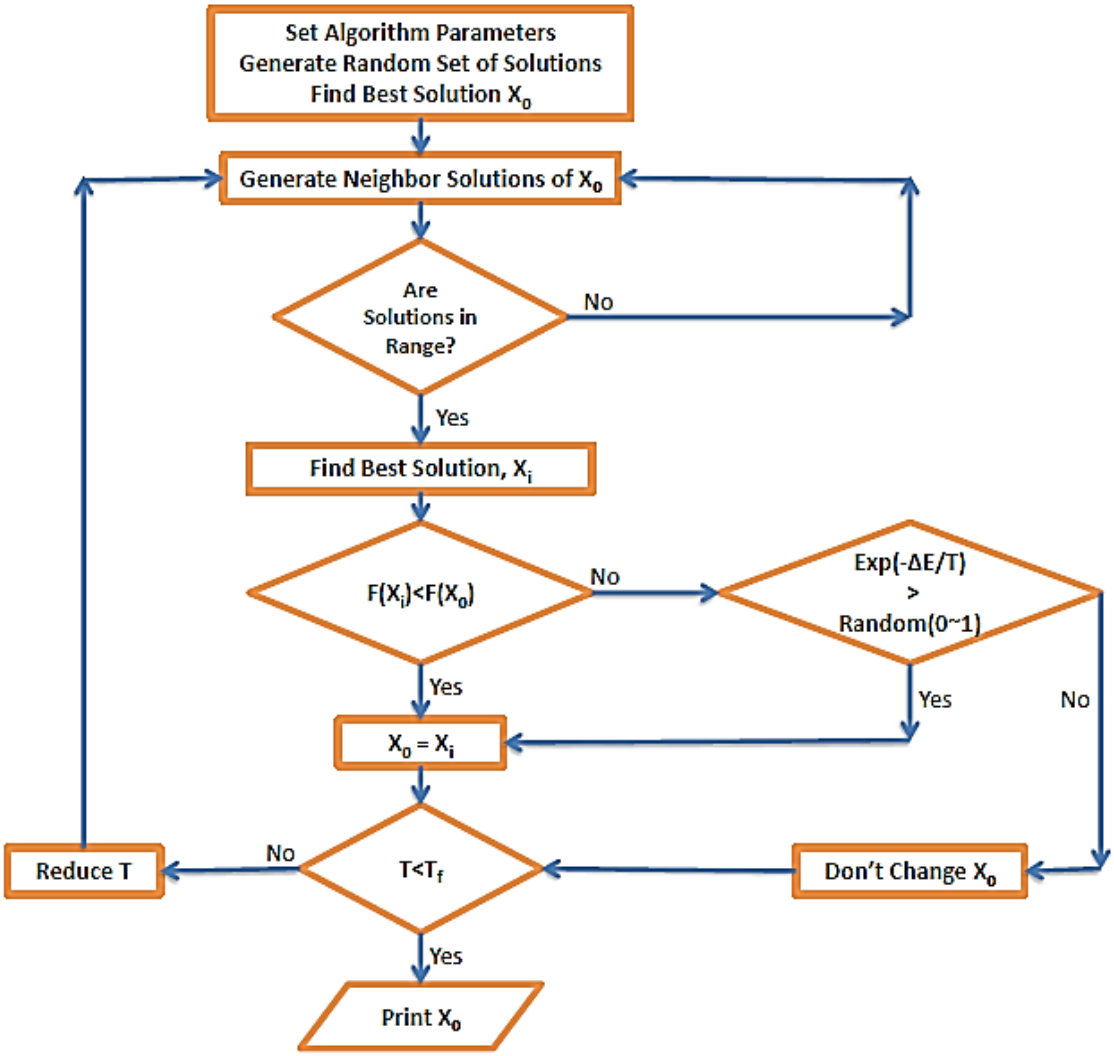

Figure 3
Flowchart of the simulated annealing algorithm (Wang et al., 2016).

As shown in Figure 3, step 1 determines the algorithm parameters. Because there is no direct way, a trial and error approach is used to determine the best algorithm parameters. Second, in step 2, a random set of constant coefficients is generated. Thirdly, using these constants, the ROP values are calculated, and the $RMSE_1$ for all the data set is determined using Equation 13. Fourthly, a neighboring set of constant coefficients is generated in step 4, and the $RMSE_2$ is determined for this new solution. In the fifth place, If $RMSE_2$ is lower than $RMSE_1$, the new solution is considered as the best solution, otherwise if *P* (Solution) > Random (0~1), the solution 2 is then considered as the best

solution. Finally, the temperature decreases ($T_{New} = \alpha \times T_{Current}$), and the process returns to step 4. The process is repeated until the freezing temperature is met.

In this study, objective function is considered as the root mean square error (RMSE). The RMSE is calculated using Equation 13.

$$RMSE = \sqrt{\frac{1}{n}\sum_{i=1}^{n}\left(ROP_{real} - ROP_{predicted}\right)^2} \tag{13}$$

Bourgoyne and Young recommended lower bound and upper bound for each of the eight coefficients. Table 2 contains recommended bounds for each of the constants (Bourgoyne et al., 1991; H Rahimzadeh et al., 2011).

Table 2
Recommended bounds for each of the constant coefficient of Bourgoyne and Young model (Bourgoyne et al., 1991; H Rahimzadeh et al., 2011).

Coefficients	Lower bound	Upper bound
a_1	0.5	1.9
a_2	0.000001	0.0005
a_3	0.000001	0.0009
a_4	0.000001	0.0001
a_5	0.5	2
a_6	0.4	1
a_7	0.3	1.5
a_8	0.3	0.6

Using a trial and error approach, the best parameters of the SAA are determined. Table 3 contains the algorithm parameters used herein.

Table 3
The best algorithm parameters.

No.	SAA parameters	Value
1	T_0	1000
2	A	0.925
3	Length of Markov chain	8
4	T_f	0.0002

Figure 4 shows the performance of the simulated annealing algorithm for determining the constant coefficients of Bourgoyne and Young model in Surmeh formation. It shows that the determined constants can predict the ROP with an RMSE value equal to 2.97318. The second diagram shows the determined constant coefficients, and the third diagram displays the final temperature. It shows that the algorithm stops when the temperature reaches the freezing temperature.

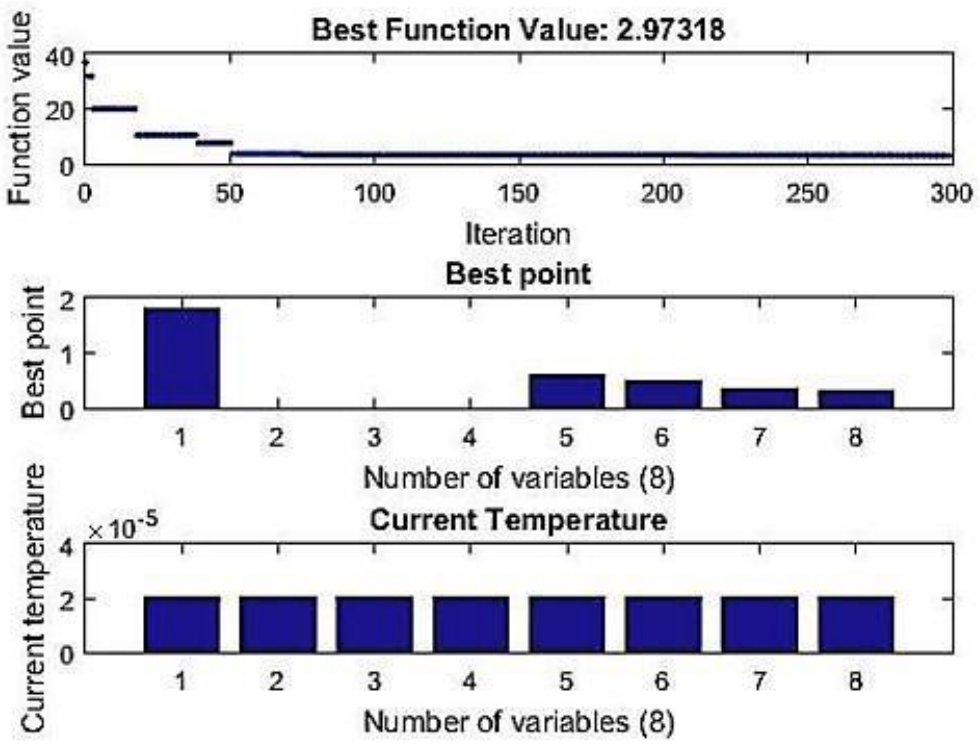

Figure 4
Performance of the simulated annealing algorithm for determining Bourgoyne and Young model in Surmeh formation.

The calculated constants are summarized in Table 4. When SAA is used for determining the constant coefficients of mathematical models, sometimes after each run, a set of completely different constants is obtained. In this situation, the parameters of the algorithm must be changed to reach the global optimum. The measured and predicted drilling rates for each formation are depicted in Figure 5.

Table 4
Bourgoyne and Young model constants for each formation.

Formation	a_1	a_2	a_3	a_4	a_5	a_6	a_7	a_8
Asmary	1.535	0.000075	0.000002	0.0001	0.595	0.94	0.895	0.49
Ilam	1.125	0.000101	0.000459	0.000002	0.5	0.405	1.4999	0.595
Sarvak	1.289	0.000079	0.000002	0.000002	0.505	0.98	0.3067	0.435
Upper limestone	1.259	0.00001	0.000043	0.000002	0.865	1	0.305	0.595
Dashtak	1.329	0.000044	0.00012	0.000002	0.505	0.95	0.301	0.3046
Surmeh	1.831	0.000021	0.0001	0.000001	0.619	0.516	0.375	0.342
Kangan	1.525	0.000001	0.000001	0.000001	0.79	0.995	0.303	0.410

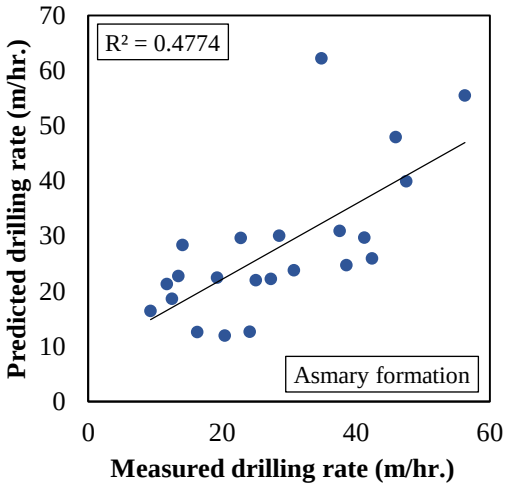
R² = 0.4774
Asmary formation
Predicted drilling rate (m/hr.)
Measured drilling rate (m/hr.)
0
10
20
30
40
50
60
70

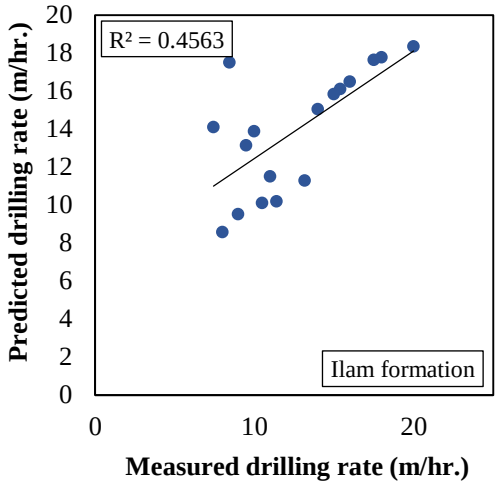
R² = 0.4563
Ilam formation
Predicted drilling rate (m/hr.)
Measured drilling rate (m/hr.)
0
2
4
6
8
10
12
14
16
18
20

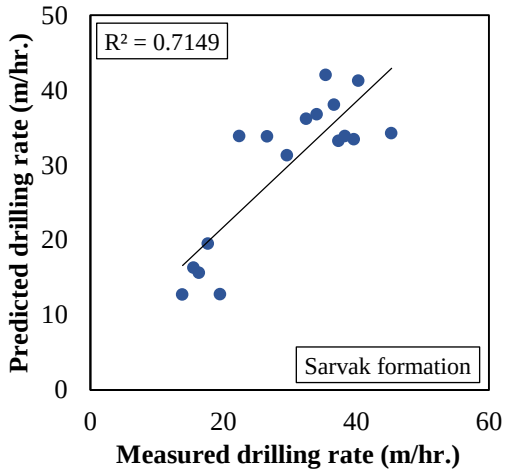
R² = 0.7149
Sarvak formation
Predicted drilling rate (m/hr.)
Measured drilling rate (m/hr.)
0
10
20
30
40
50
60

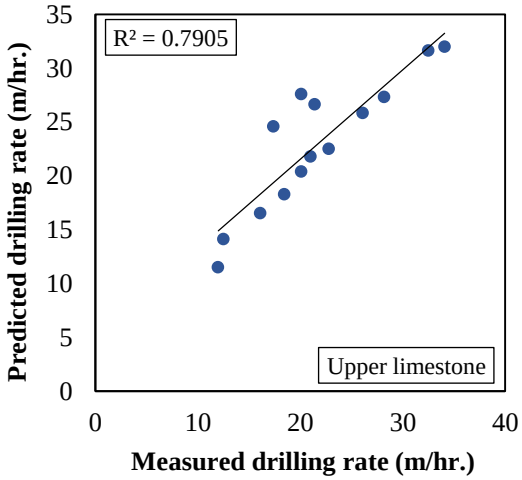
R² = 0.7905
Upper limestone
Predicted drilling rate (m/hr.)
Measured drilling rate (m/hr.)
0
5
10
15
20
25
30
35
40

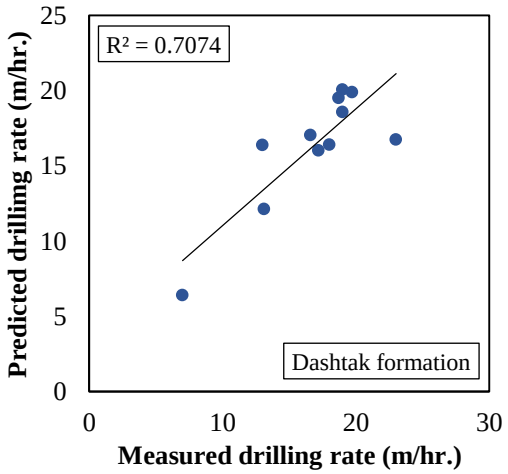
R² = 0.7074
Dashtak formation
Predicted drillimg rate (m/hr.)
Measured drilling rate (m/hr.)
0
5
10
15
20
25
30

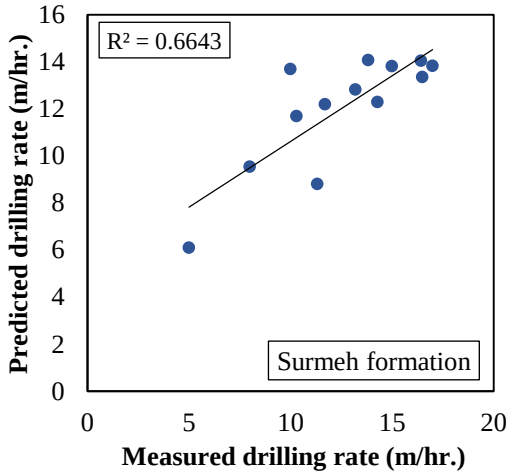
R² = 0.6643
Surmeh formation
Predicted drilling rate (m/hr.)
Measured drilling rate (m/hr.)
0
2
4
6
8
10
12
14
16
20

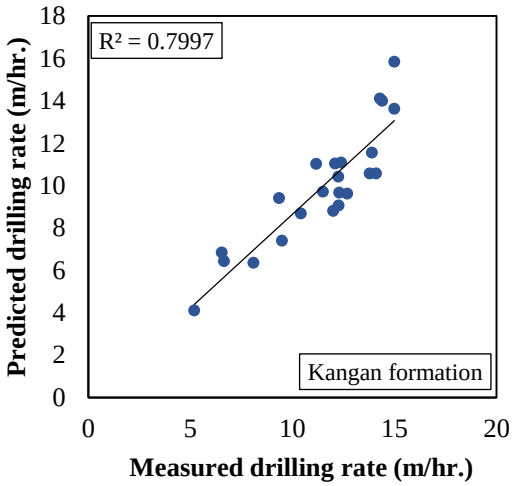

Figure 5
Measured versus predicted drilling rate for each formation by Bourgoyne and Young model.

4. Hareland-Rampersad (HR) model

In 1994, Hareland and Rampersad established a model to predict the drilling rate. This model is derived using the conservation of mass where the rate of cutting removal is equivalent to the rate of penetration (Hareland et al., 1994). The general form of the model for completely efficient bit cleaning is as follows:

$$ROP = W_f \left(\frac{G \cdot WOB^{\alpha} \cdot RPM^{\gamma}}{D_{Bit} \cdot \sigma} \right) \tag{14}$$

where, ROP (ft./hr.) is the predicted rate of penetration, and WOB (lb) is weight on bit; RPM is the rotary speed of bit in revolution per minute; G stands for a constant coefficient which is related to bit type and blade geometry, and D_{Bit} (in) denotes bit diameter; σ (psi) is the uniaxial compressive strength (UCS) of the rock, and a and γ are model constants; w_f indicates the wear function. Wear function calibrates the ROP for a worn bit. The wear function is calculated using Equation 15 as a function of cumulative bit wear. The cumulative bit wear is a function of applied RPM and WOB, rock strength, and length of drilling interval:

$$W_f = 1 - \left(1 - \frac{\Delta BG}{8}\right)^{w} \tag{15}$$

where, ΔBG is the IADC bit dull grading estimated by Equation 16:

$$\Delta BG = C_a \cdot \sum_{i=1}^{n} RPM^{c_1} \cdot \left(\frac{WOB}{1000}\right)^{c_1} \cdot \left(\frac{\sigma}{1000}\right) \cdot x_i \tag{16}$$

In above equation, C_a represents the bit wear coefficient and is a function of the durability of PDC layer material and the relative hardness of the cutters with respect to the PDC layer material (Liu et al., 2014). c_1 and c_2 are model constants, and x_i is the length of drilling interval in feet. By assuming a linear relation for the bit wear function, w_f is given by (Hedayat Rahimzadeh et al., 2010):

$$W_f = 1 - \left(\frac{\Delta BG}{8}\right) \tag{17}$$

where,

$$\Delta BG = C_a \cdot \sum_{i=1}^{n} RPM \cdot \left(\frac{WOB}{1000}\right) \cdot \left(\frac{\sigma}{1000}\right) \cdot x_i \tag{18}$$

In this model, the uniaxial compressive strength of the rock is obtained using empirical correlations which are a function of bulk density and sonic wave transit time. The same data set, which is used to construct Bourgoyne and Young model, is utilized to obtain Hareland model constants in each formation. For the calculation of C_a, the summation term in Equation 18 is calculated using drilling data extracted from MLDR; then, the IADC bit dull grading term is divided by that summation to provide the value of C_a. In addition, Hareland-Rampersad model has three constants; for determining these constants, the model needs to be linearized. The linear form of the HR model is written by Equations19-20. The formulas for calculating the HR coefficients of X and Y are given in Table 5.

$$Y = a_1 + a_2 X_1 + a_3 X_2 \tag{19}$$

$$Ln\left(\frac{ROP.D_{Bit}.\sigma}{W_f}\right) = Ln(G) + \alpha Ln(WOB) + \gamma Ln(RPM) \tag{20}$$

Table 5
Coefficients of linear form of Hareland-Rampersad model.

Characteristic	Variable	Amount
Drilling rate parameter	Y	$Ln\left(\frac{ROP.D_{Bit}.\sigma}{W_f}\right)$
Weight on b parameter	X_1	$Ln(WOB)$
Rotary speed parameter	X_2	$Ln(RPM)$
Constant coefficient	a_1	$Ln(G)$

Then, X and Y values are determined using the data set, so MLR matrix is constructed. By solving the MLR matrix, the constants are determined. When MLR leads to negative constants, SAA can be employed to determine the constants. Table 6 contains the recommended ranges of Hareland-Rampersad model constants.

Table 6
Recommended bounds of Hareland-Rampersad model constants.

Coefficients	Lower bound	Upper bound
G	0.1	100
α	0.5	1.5
γ	0.5	1.5

The model constants for each formation are summarized in Table 7. Figure 6 shows the measured and predicted drilling rate acquired by Hareland model with the best fit line and R^2 values for different formations of the SP gas field.

Table 7
Hareland model constants for each formation.

Formation	*G*	*α*	*ɣ*	C_a
Asmary	0.00521673	1.3982	0.9025	1.53E-6
Ilam	53.489	0.5858	0.9887	3.4E-7
Sarvak	7.198	0.6113	1.2944	1.72E-7
Upper limestone	50.436	0.7473	0.7163	9.32E-8
Dashtak	50.6	0.5944	1.0074	3.06E-8
Surmeh	54.535	0.6948	0.8687	6.11E-8
Kangan	53.425	0.79568	0.63118	1.68E-8

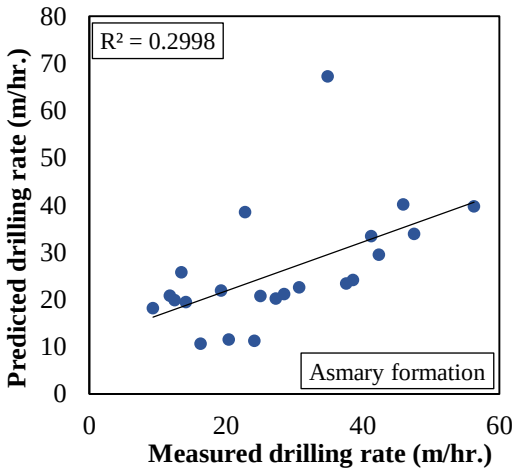

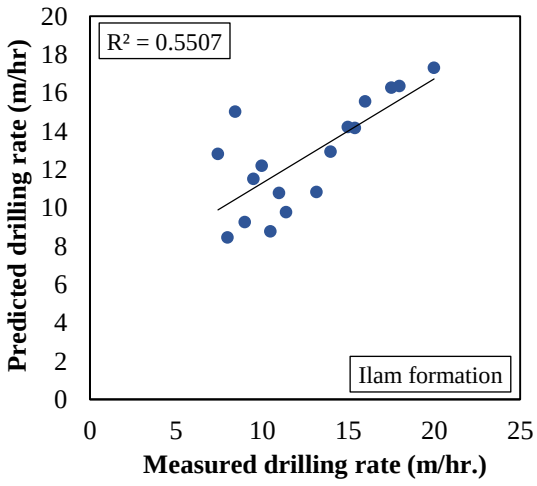

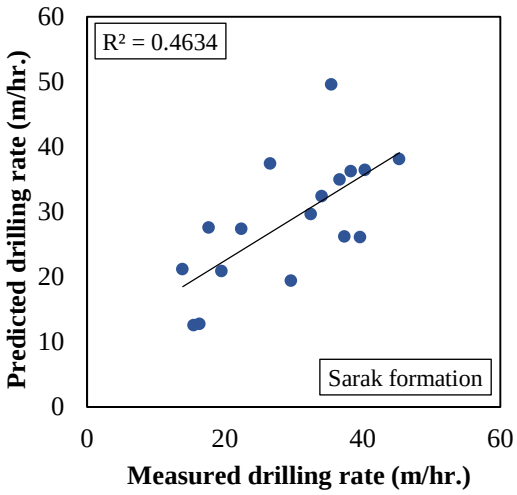

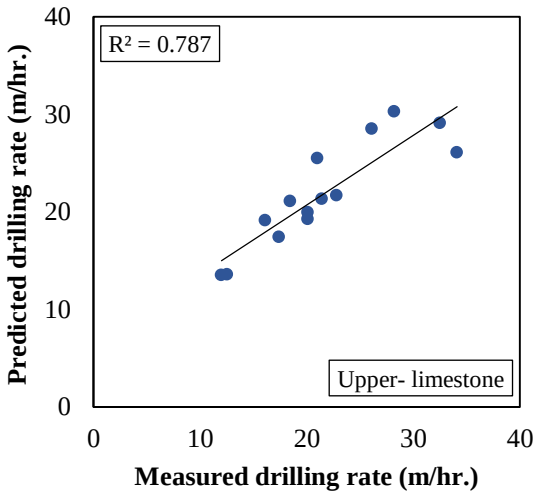

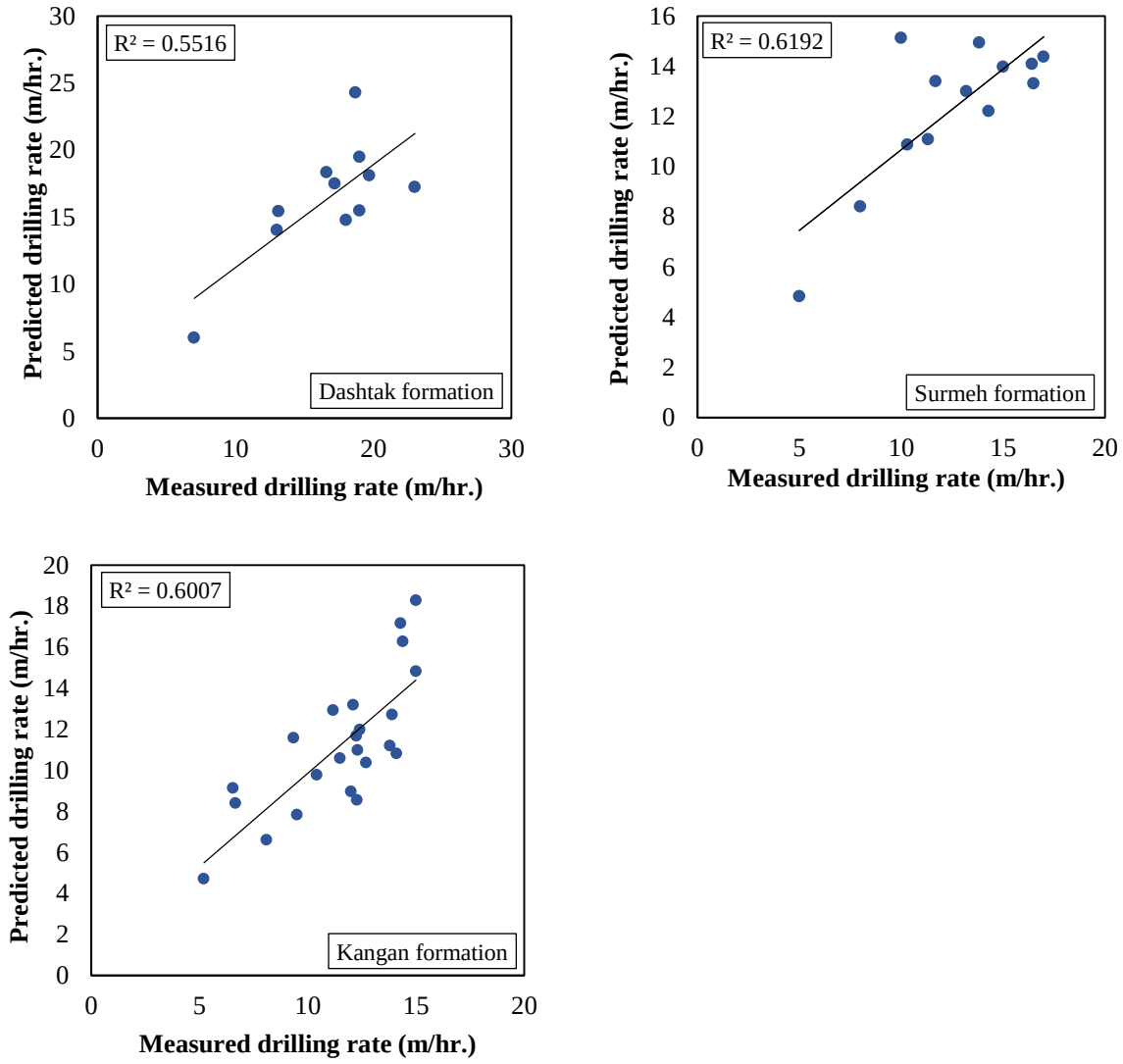

Figure 6
Measured versus predicted drilling rate for each formation by Hareland model.

Artificial intelligence models

Previous researches proved that ANN can predict ROP accurately within the range of input data when a large data set is available. Table 8 contains the drill-off test data of Surmeh formation in a 12.25 inch hole section which was drilled with a PDC bit. The mud weight and flowrate were equal to 9.6 ppg 870 gpm respectively. The ANN and ANFIS are employed to construct a model for the prediction of ROP using the drill-off test data.

Table 8
Drill-off test data of Surmeh formation.

WOB (klb)	5	8	11	13	14	15	17	14	14	14	14
RPM (rpm)	180	180	180	180	180	180	180	190	200	210	220
ROP (m/hr.)	5.5	9.12	13.46	14	14.21	13.5	13.09	15.31	16.5	17.35	18

The WOB and RPM are considered as the input variables, and ROP is the output of the model. The available data sets consisted of 80% for the pure network learning process, 10% for validation, and 10% for testing purposes. A two-layered feed-forward back propagation algorithm with 10 neurons in the hidden layer is used. The Levenberg-Marquardt (LM) algorithm is selected for training the network. Figure 7 shows the structure of the designed ANN model.

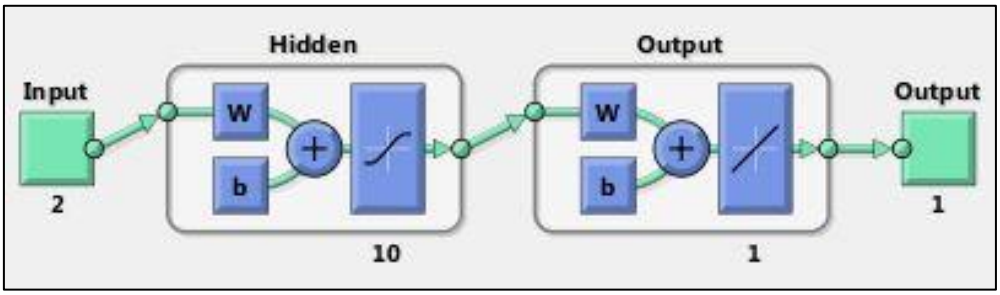

Figure 7
Structure of the suggested ANN for the prediction of ROP.

Figure 8 shows the relationship between WOB, RPM, and ROP using the constructed ANN model. As it is seen, the ANN is able to predict the ROP only within the range of the input data, and when there is not enough input data with a sufficient distribution, it cannot be used as a reliable model for the prediction of ROP.

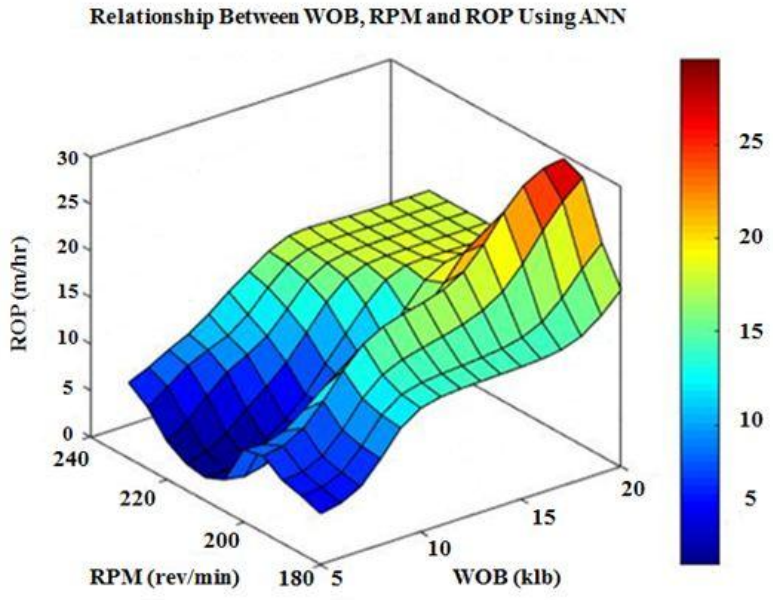

Figure 8
Relationship between WOB, RPM, and ROP using the designed ANN model.

Following this, ANFIS is used to construct a model for the prediction of ROP using the drill-off test data. WOB and RPM are the input variables, and ROP is the output of the model. The data used to construct the ANFIS are the same as ANN: 80% for training, 10% for testing, and 10% for checking purposes. The type of membership functions is selected as a Gaussian curve, and three membership functions are chosen for each linguistic variable. Figure 9 shows the structure of the designed ANFIS model.

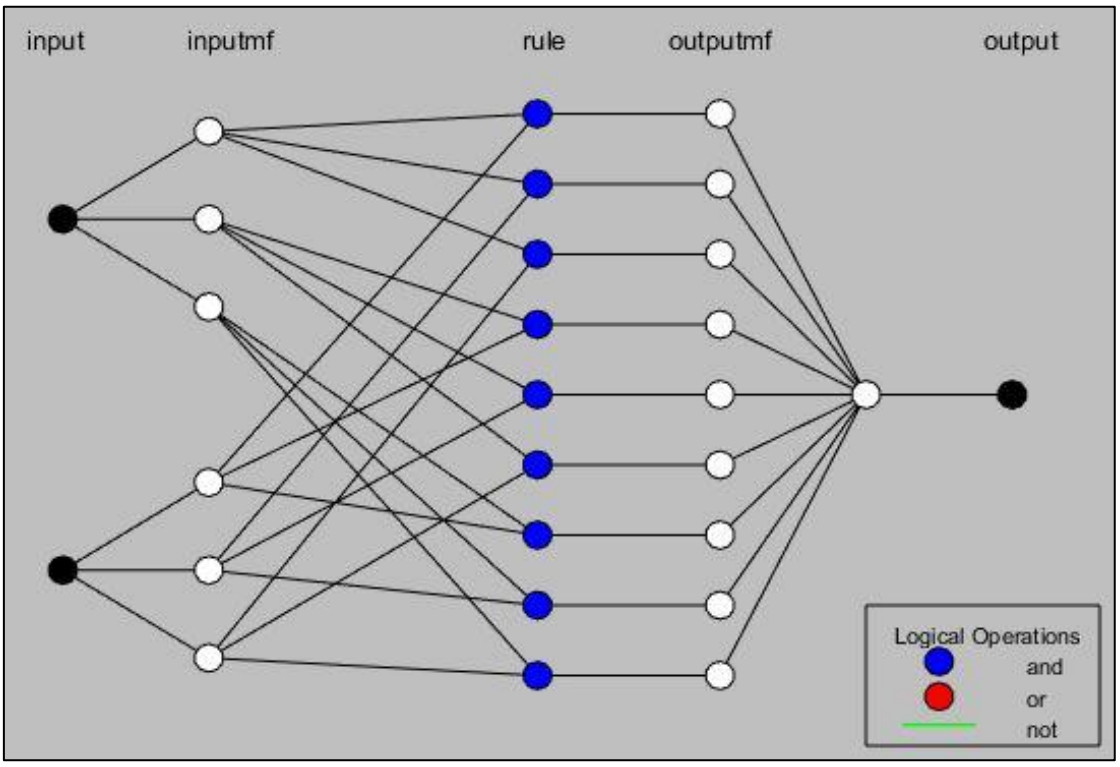

Figure 9
Structure of the designed ANFIS model for the prediction of ROP.

Figure 10 shows the relationship between WOB, RPM, and ROP using the designed ANFIS model. It is noticeable that ANFIS has better performance than ANN in a way that it can be used as a reliable model for the prediction of ROP when a few numbers of input data with a sufficient distribution are available.

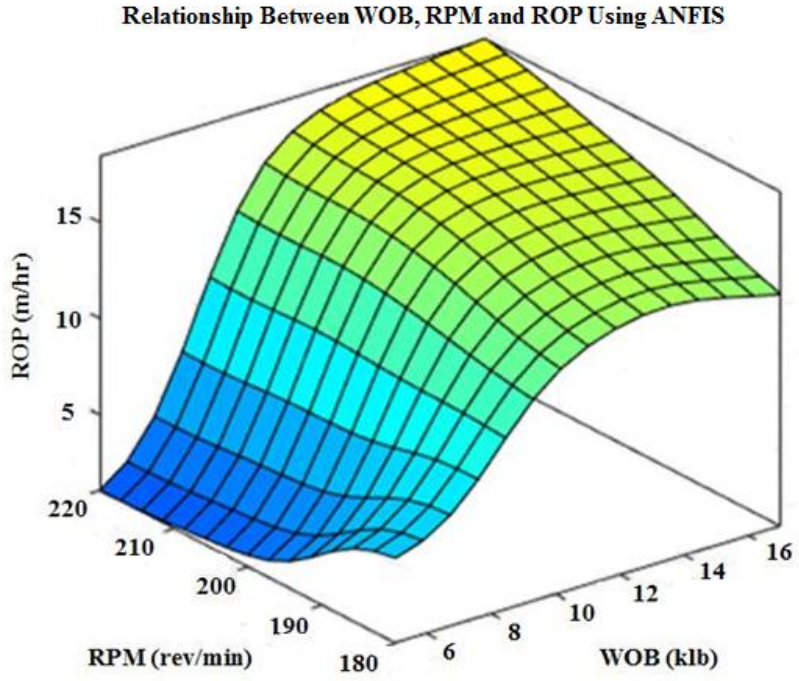

Figure 10
Relationship between WOB, RPM, and ROP using the designed ANFIS model.

It can be concluded that in cases in which a vast amount of data set are not available, using ANFIS instead of ANN can lead to more accurate and reliable results.

5. Theoretical basis and justification for ANFIS applied to ROP prediction models

The models which are based on fuzzy-inference system use linguistic terms and if-then rules instead of numerical terms. Linguistic variables have their values expressed as words or sentences of natural language describing degrees of membership. A fuzzy set, which belongs to these linguistic variables, is an extension of a crisp set where each element can have binary membership, i.e., full membership or no membership. However, fuzzy sets allow partial membership in which an element can partially belong to one or more than one set (Nedjah et al., 2005). In other words, in a crisp set, the membership level of *x* elements in set A can be expressed by the membership function $\mu_A(x)$, such that if:

$$\mu_A(x) = \begin{cases} 1 & if\ x \in A \quad implying\ full\ membership \\ 0 & if\ x \notin A \quad implying\ non-membership \end{cases} \tag{21}$$

where, for fuzzy set A, membership function $\mu_A(x)$ has values between 0, 1.

In ANFIS, input data are converted to fuzzy input by membership functions. Following this, fuzzy inputs are entered into the neural network block. This block is connected to an inference engine which includes a rule base. A back-propagation algorithm is used to train the inference engine and to determine appropriate rules that can reproduce meaningful dependent variable values. After training, the rules generated are applied to the dataset from the neural network to yield the optimum output. Then, the output which is obtained from the neural network block is converted into crisp values by a defuzzification algorithm (Sugeno et al., 1988). This analytical sequence is shown in Figure 11. There are five layers in the structure of neuro-fuzzy system; these layers are fuzzification, rules, normalization, defuzzification, and output as shown in Figure 12. Each of these layers includes nodes, which processes the fuzzy inputs. Since the ANFIS only allows one model output, the outputs of these nodes are combined to yield a single crisp output. Then, the derived output is reentered as an input to the model and compared with the actual set value. If there is any deviation, the error signal is generated and becomes the input to the next iteration of the ANFIS model. Following a series of iterations, results converge to a stable system with minimal errors between the predicted and measured values (Mathur et al., 2016).

The Takagi, Sugeno, and Kang (TSK) fuzzy inference system is used to construct the ANFIS model, which consists of two rules (Sugeno et al., 1988). The TSK ROP model involves two inputs *WOB* and *RPM*, one output ROP, and fuzzy sets $A_1.A_2.B_1.B_2$. A and B are fuzzy sets of variables *WOB* and *RPM* respectively. In the ANFIS model, the relation between the inputs and output is expressed by the following *If-Then* rules:

Rule 1: $if\ WOB\ is\ A_1\ and\ RPM\ is\ B_1;\ then\ ROP_1 = p_1\,WOB + q_1\,RPM + r_1$

Rule 2: $if\ WOB\ is\ A_2\ and\ RPM\ is\ B_2;\ then\ ROP_2 = p_2\,WOB + q_2\,RPM + r_2$

where, p_1 , q_1 , r_1 , p_2 , q_2 , and r_2 are consequent parameters. $A_1.A_2.B_1.B_2$ are the fuzzy sets which represent the linguistic labels. Each layer in the ROP ANFIS model consists of the following node functions:

Layer 1: This layer is the fuzzification layer. In this layer, the crisp value enters into node i which is converted into a fuzzy value associated with fuzzy set A_i or B_i. Then, the membership level of this

input is determined by a membership function of the respective fuzzy set. The output of each node is calculated by using the following equations:

$$O_{1.i} = \mu_{Ai}(WOB) \quad for\ i = 1.2 \tag{22}$$

$$O_{1.i} = \mu_{Bi}(RPM) \quad for\ i = 1.2 \tag{23}$$

Layer 2: This layer is the first rule layer. The nodes of this layer are fixed, and they multiply the membership levels of all the inputs according to each rule as follows:

$$O_{2.i} = w_i = \mu_{Ai}(WOM)\mu_{Bi}(RPM) \quad for\ i = 1.2 \tag{24}$$

where, $O_{2.i}$ denotes the output of layer 2, and w_i is the firing strength. In this layer, each node calculates the firing strength of each rule via multiplication, and the rule which has the high firing strength matches the input data. The number of nodes is equal to the number of rules in this layer.

Layer 3: This layer is the second rule layer. In this layer, each node calculates the ratio of firing strength of each rule to the sum of all rules. The firing strength is calculated by:

$$O_{3.i} = \overline{w_i} = \frac{w_i}{w_1 + w_2} \quad for\ i = 1.2 \tag{25}$$

where, $\overline{w_i}$ represents normalized firing strength.

Layer 4: This layer is the defuzzification layer. The node function in this layer is calculated as follows:

$$O_{4.i} = \overline{w_i} \times ROP_i = \overline{w_i} \times (p_i\, WOB + q_i\, RPM + r_i) \quad for\ i = 1.2 \tag{26}$$

where, $\overline{w_i}$ is normalized firing strength calculated from layer 3, and ROP_i can be a polynomial function or constant number. $\{p_i.\, q_i.\, r_i\}$ is a consequent parameter set for rule i (Jang, 1993).

Layer 5: This layer is the output layer. It only has one node, and this node calculates the sum of the output of all the nodes from layer 4 to produce the overall ANFIS output as reads:

$$overall\ output = O_{5.i} = \sum_i \overline{w_i} ROP_i = \frac{\sum_i w_i ROP_i}{\sum_i w_i} \quad for\ i = 1.2 \tag{27}$$

This ROP ANFIS model developed using the training data subset is then used to predict the rate of penetration for each data set record of the test subset so as to determine its accuracy.

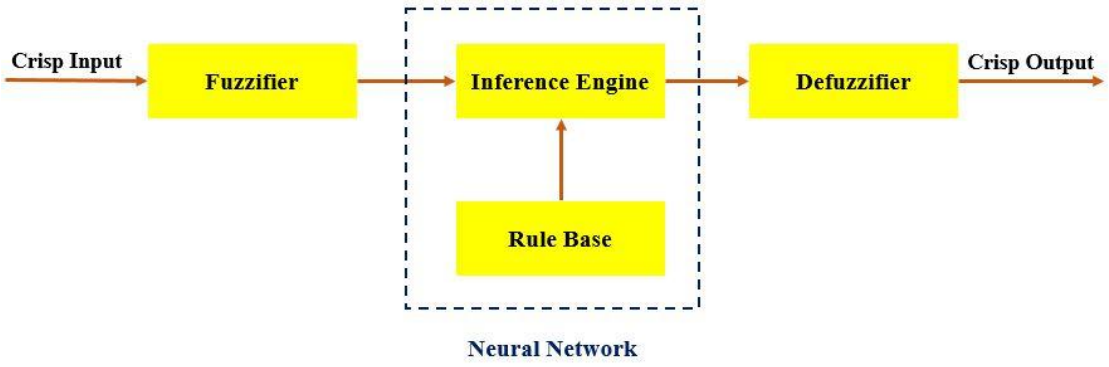

Figure 11
A high-level schematic for the sequence involved in a fuzzy neural network (Mathur et al., 2016).

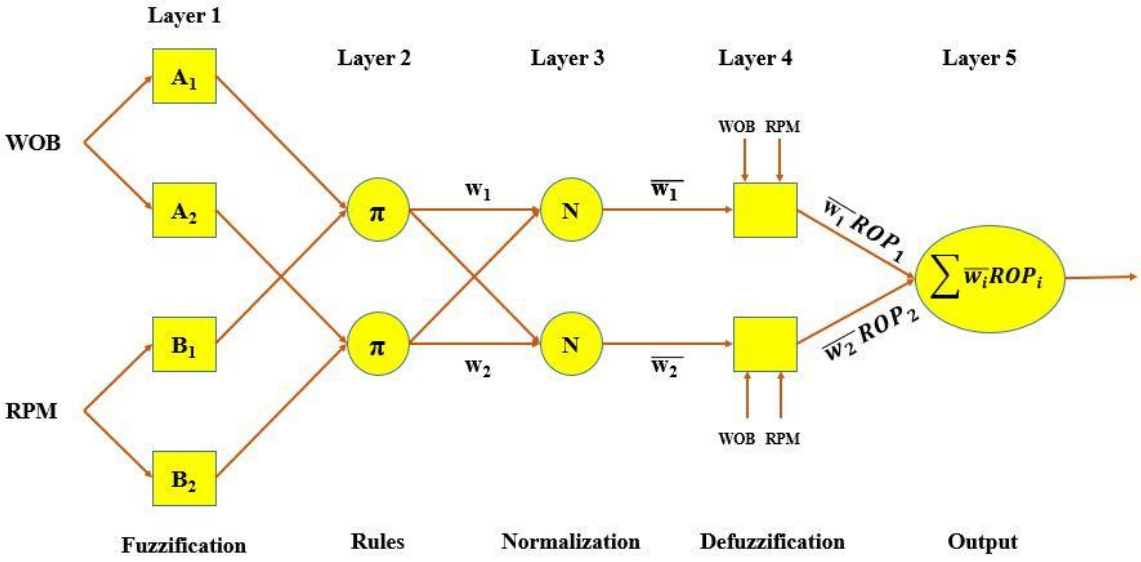

Figure 12
ANFIS architecture involving two rules and two inputs.

5.1 Prediction of drilling rate by ANFIS

The same data set which is used for the two previous mathematical ROP models (i.e., BY and HR models) is utilized to construct the ANFIS model. After the classification of the data set, the ANFIS model is trained using MATLAB software. The Takagi, Sugeno and Kang (TSK) fuzzy inference system is used to construct the ANFIS model, and a hybrid rule algorithm is utilized to train the adaptive network. Model inputs include depth, weight on bit, rotational speed, flow rate, mud weight, pore pressure, and bit wear, and the only output is the rate of penetration. In the developed model, three-membership functions are considered for each input data record. The type of membership functions is *trimf* membership function which consists of three constants. The linguistic expressions for the input data, except for bit type, are low (L), moderate (M), and high (H). These linguistic labels state the relation between the input and output data via fuzzy *If-Then* rules. The linguistic labels and corresponding membership functions for the Sarvak formation are summarized in Table 9.

In this study, *If-Then* rules are created according to the relationship between the input and output for each record of the training subset of the data set. The created rule-base contains 2187 rules, and a sample of these rules is given by:

Rule 1:

$$if\ Depth\ is\ L\ and\ WOB\ is\ H\ and\ RPM\ is\ H\ and\ flow\ rate\ is\ H\ and\ mud\ weight\ is\ L$$

$$and\ pore\ pressure\ is\ L\ and\ bit\ wear\ is\ L, then\ ROP_1 = f(depth.WOB\ \ldots)\ is\ H$$

The last step is defuzzification and drilling ROP is converted from a fuzzy expression into a crisp value. A plot of the predicted and measured penetration rates together with the best fit line and correlation coefficient (R^2) values for testing data set is given in Figure 13.

Table 9
Linguistic labels and corresponding membership functions for the Sarvak formation.

Parameter	Linguistic term	Parameters of membership function		
		a	***b***	***c***
TVD	Low	827.5	995	1162.5
	Moderate	995	1162.5	1330
	High	1162.5	1330	1497.5
WOB	Low	-2.45	4.6	11.65
	Moderate	4.6	11.65	18.7
	High	11.65	18.7	25.75
RPM	Low	8.5	85	161.5
	Moderate	85	161.5	238
	High	161.5	238	314.5
Flow rate	Low	2718.5	3312	3905.5
	Moderate	3312	3905.5	4499
	High	3905.5	4499	5092.5
Mud weight	Low	9.41	9.41	9.41
	Moderate	9.41	9.41	9.41
	High	9.41	9.41	9.41
Pore pressure	Low	8.51	8.51	8.51
	Moderate	8.51	8.51	8.51
	High	8.51	8.51	8.51
Bit wear	Low	-0.101	0.0161	0.1332
	Moderate	0.0161	0.1332	0.2503
	High	0.1332	0.2503	0.3674

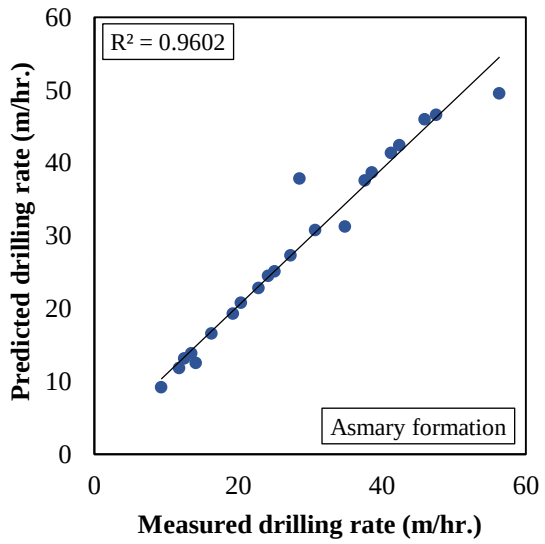

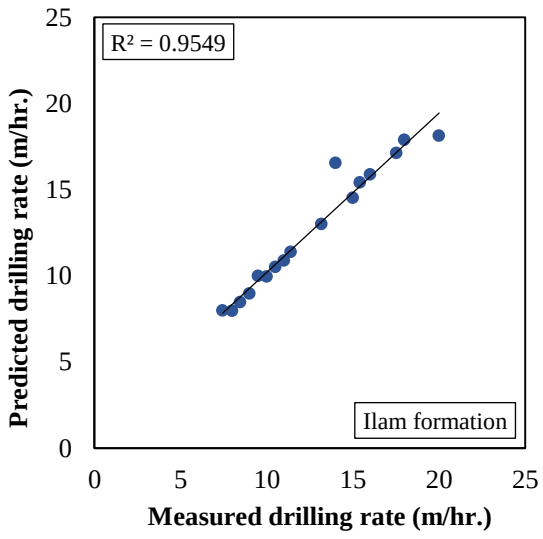

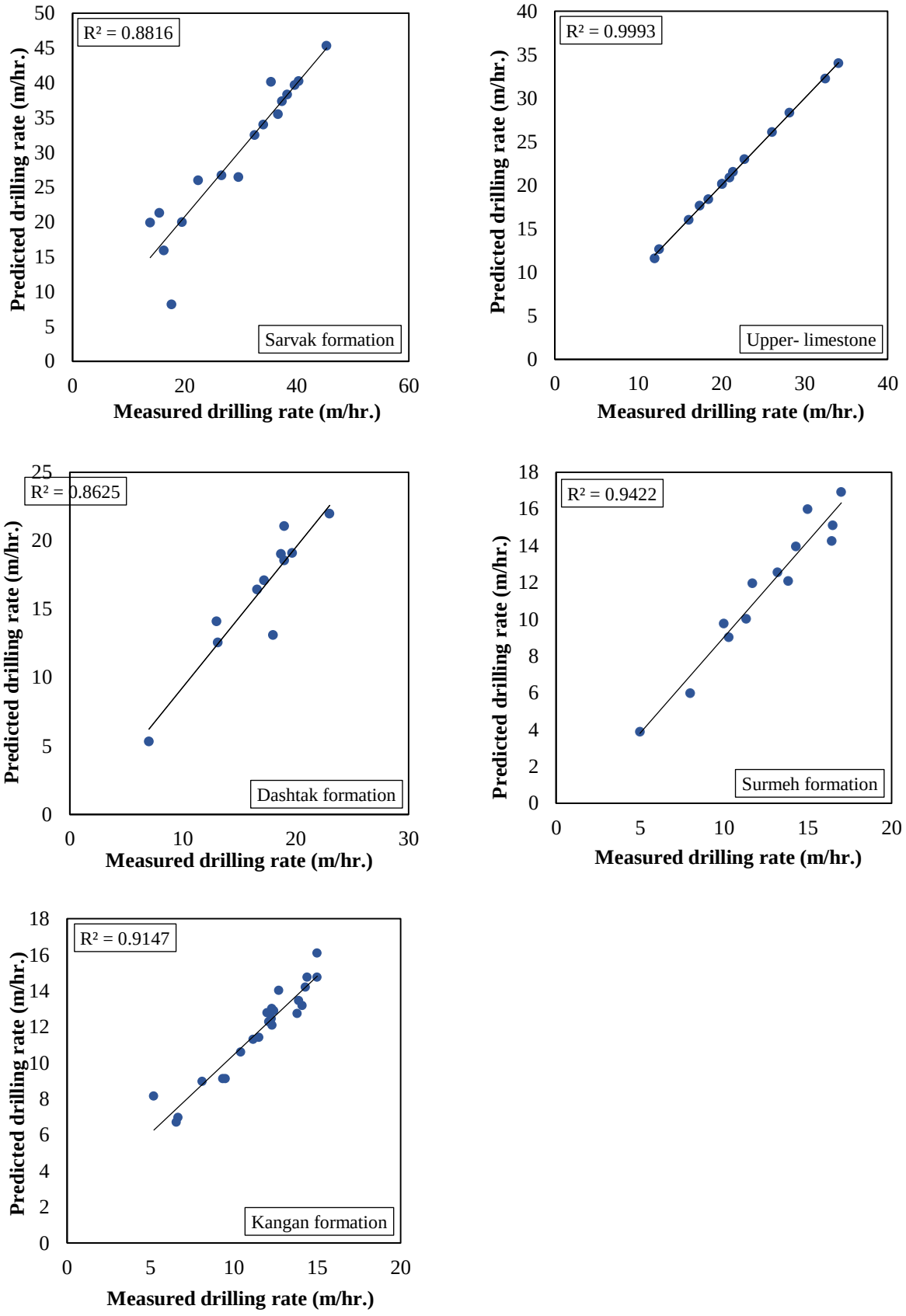

Figure 13
Measured versus predicted drilling rate for each formation applying the ANFIS ROP model.

6. Model performance analysis

According to the results obtained by the ANFIS model, this model has the least amount of error compared to Bourgoyne and Young and Hareland-Rampersad models; its average error is less than 10% in all the studied formations. Therefore, the ANFIS ROP model can be considered as the most appropriate tool to predict the drilling ROP. Figure 14 shows the measured and predicted values of ROP using the three different models evaluated. In addition, the amount of the residual error for each of the developed models is shown in Figure 15. Clearly, the residual errors yielded by the ANFIS ROP model are lower than the ones of the other two widely used ROP models. In other words, the deviation of the predicted values from the measured values is less in ANFIS. Analytical models consider the effect of a limited number of parameters to predict the drilling rate. On the other hand, there is no limitation for the number of input variables in ANFIS, and the effect of any variables on drilling ROP can be considered and included. For this reasons, ANFIS has the best performance in all the studied formations.

It is worth noting that the artificial intelligence systems such as adaptive-neuro-fuzzy-inference system work better than other approaches when a large amount of data exists. In situations where a large number of data records are not available to train such models, conventional mathematical methods are likely to be superior to inference systems. On the other hand, ANFIS can predict ROP accurately within the range of input data, but it is not able to predict the ROP beyond the range of input data; however, mathematical ROP models can predict the ROP in all ranges, and they need less input data compared to ANFIS.

Overall, it can be seen that Bourgoyne and Young model has a better performance than the Hareland-Rampersad model in most of the formations. Since the effect of different parameters such as pore pressure, mud weight, flow rate, and bit nozzle size are considered in Bourgoyne and Young model, it works better than Hareland-Rampersad model in the prediction of drilling ROP.

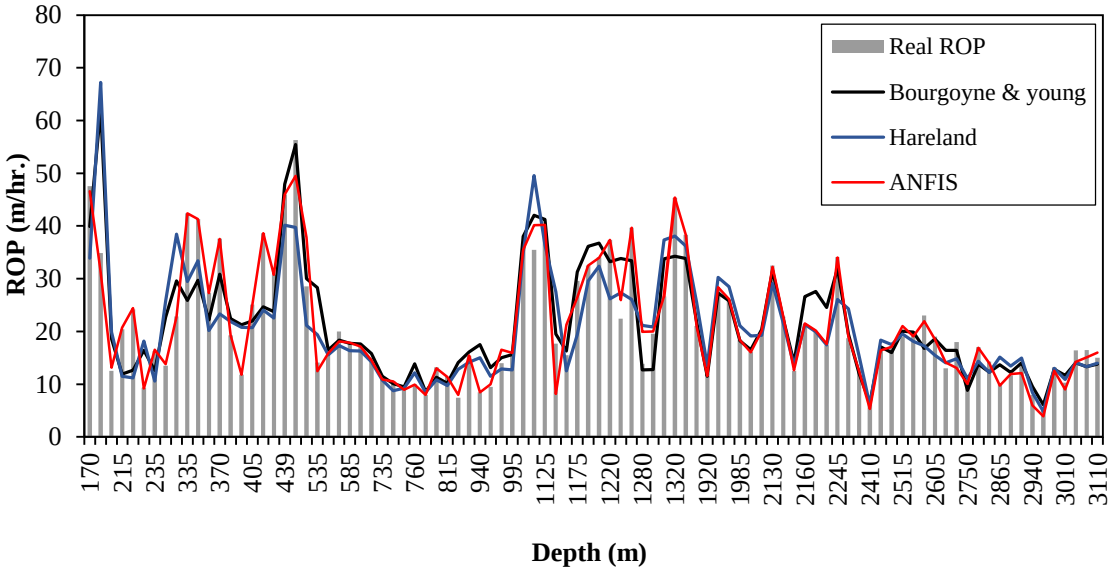

Figure 14
Measured and predicted drilling rates using different approaches.

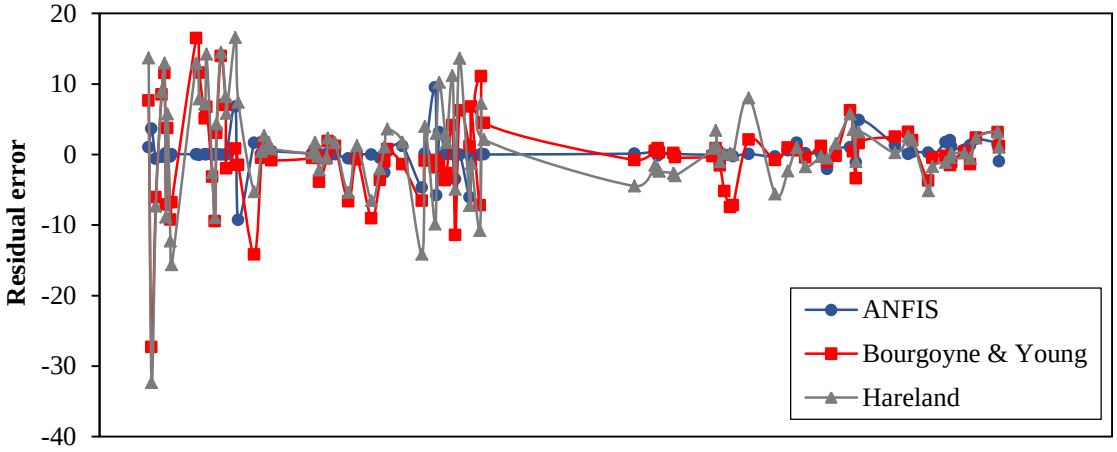

Figure 15
Residual errors of predicted values by ANFIS, Bourgoyne and Young, and Hareland models.

On the other hand, Hareland-Rampersad model is more accurate than Bourgoyne and Young model in Upper-limestone and Surmeh formations as can be seen in Table 10. In these formations, the pore pressure, mud weight, and mud flow rate have very little variations, while the uniaxial compressive strength (UCS) of these formations is variable. The Hareland-Rampersad model considers the effect of UCS, which has a significant impact on the rate of penetration, whereas the Bourgoyne and Young model considers a constant value of drillability for these formations. For this reason, the Hareland-Rampersad model has a better prediction performance than Bourgoyne and Young model for those two formations. It can be concluded that Hareland-Rampersad ROP model in formations where the pore pressure, flow rate, and mud weight do not vary significantly is a more appropriate choice compared to the Bourgoyne and Young model; nevertheless, both are inferior to the ANFIS ROP model developed here.

Table 10
Average percentage error for ANFIS, Bourgoyne and Young, and Hareland-Rampersad models for each formation.

Formation type	ANFIS model (%)	Bourgoyne and Young model (%)	Hareland model (%)
Asmary	3.75	36.91	43.49
Ilam	3.01	13.93	17.96
Sarvak	10.79	14.88	23.97
Upper-limestone	0.75	10.18	9.73
Dashtak	8.01	9.17	13.99
Surmeh	9.64	15.15	12.45
Kangan	6.32	14.44	16.24

7. Conclusions

In this study, the adaptive neuro-fuzzy inference system and two most-widely used mathematical ROP models (i.e. Bourgoyne and Young and Hareland-Rampersad models) are used to predict the rate of penetration in the SP gas field. A comparison of the results suggests the following conclusions:

- When a few numbers of input data are available, the ANN cannot be used for the prediction of ROP. ANFIS uses a combination of fuzzy logic and neural network, which helps ANFIS to

have a better performance than ANN, especially when a few numbers of input data are available.

- ANFIS is an accurate tool for the prediction of ROP, but the performance of ANFIS depends on various factors such as the number, accuracy, and distribution of input data and the type of membership functions. Since there is no direct way to determine the proper membership functions, trial and error should be used for this purpose. It is worth noting that this method is time consuming, especially when the number of input variables increases, and sometimes it is not possible to construct a reliable model for the prediction of ROP using ANFIS.
- Although mathematical ROP models are less accurate than ANFIS, they need less data to be constructed and always provide a reasonable estimation of ROP. Therefore, it is better to use ANFIS and mathematical ROP models simultaneously for the prediction of drilling rate in a particular formation.
- Overall, Bourgoyne and Young model has better performance than Hareland-Rampersad model in the prediction of drilling rate.
- In formations where some parameters such as mud weight, mud flow rate, and pore pressure gradients do not change significantly, Hareland-Rampersad model is a better choice for the prediction of drilling ROP compared to Bourgoyne and Young model.

Acknowledgments

The authors would like to thank National Iranian Drilling Company (NIDC) for supporting this work, for providing the mud logging data, and for permitting the publication of the results of the project.

Nomenclature

ANFIS	: Adaptive neuro-fuzzy inference system
ANN	: Artificial neural network
BG	: IADC bit dull grading
BY	: Bourgoyne and Young model
C_a	: Bit wear coefficient
D	: True vertical depth (ft.)
d_b	: Bit diameter (in)
E	: Energy function
ECD	: Equivalent circulation density (ppg)
f	: Bourgoyne and Young model functions
FIS	: Fuzzy inference system
F_j	: Jet impact force (lb_f)
G	: Constant coefficient of Hareland model
h	: Bit wear
HR	: Hareland model
L	: Length of Markov chain
N	: Rotary speed at Bourgoyne and Young model (rpm)
O	: Output of each node in ANFIS
ROP	: Rate of penetration (ft./hr.)
RPM	: Rotary speed (rpm)
SAA	: Simulated annealing algorithm
T_0	: Initial temperature (°C)
T_f	: Freezing temperature (°C)

UCS	: Uniaxial compressive strength of the rock (psi)
w_f	: Wear function
WOB	: Weight on bit (klb)
X,*y*	: Variables
a	: Constant coefficients of Bourgoyne and Young model
α	: Temperature decrement factor at SAA
α & γ	: Hareland model constants
μ	: Membership function
σ	: Uniaxial compressive strength of the rock (psi)

References

Afshari, A., Shadizadeh, S., and Riahi, M., The Use of Artificial Neural Networks in Reservoir Permeability Estimation from Well Logs: Focus on Different Network Training Algorithms, Energy Sources, Part A: Recovery, Utilization, and Environmental Effects, Vol. 36, No. 11, p. 1195-1202, 2014.

Aghajanpour, A., Fallahzadeh, S. H., Khatibi, S., Hossain, M. M., and Kadkhodaie, A., Full Waveform Acoustic Data as an Aid in Reducing Uncertainty of Mud Window Design in the Absence of Leak-off Test, Journal of Natural Gas Science and Engineering, Vol. 45, p. 786-796, 2017.

Ahmadi, M. A. and Shadizadeh, S. R., New Approach for Prediction of Asphaltene Precipitation Due to Natural Depletion by Using Evolutionary Algorithm Concept, Fuel, Vol. 102, p. 716-723, 2012.

Ahmadi, M. A. and Shadizadeh, S. R., Intelligent Approach for Prediction of Minimum Miscible Pressure by Evolving Genetic Algorithm and Neural Network, Neural Computing and Applications, Vol. 23, No. 2, p. 1-8, 2013.

Alexeyev, A., Ostadhassan, M., Mohammed, R. A., Bubach, B., Khatibi, S., Li, C., and Kong, L., Well Log Based Geomechanical and Petrophysical Analysis of the Bakken Formation, 2017.

Ansari, H. R., Hosseini, M. J. S., and Amirpour, M., Drilling Rate of Penetration Prediction Through Committee Support Vector Regression Based on Imperialist Competitive Algorithm, Carbonates and Evaporites, Vol. 32, No. 2, p. 205-213, 2016.

Arabjamaloei, R. and Shadizadeh, S., Modeling and Optimizing Rate of Penetration Using Intelligent Systems in an Iranian Southern Oil Field (Ahwaz Oil Field), Petroleum Science and Technology, Vol. 29, No. 16, p. 1637-1648, 2011.

Asoodeh, M., Shadizadeh, S., and Zargar, G., The Estimation of Stoneley Wave Velocity from Conventional Well Log Data: Using an Integration of Artificial Neural Networks, Energy Sources, Part A: Recovery, Utilization, and Environmental Effects, Vol. 37, No. 3, p. 309-317, 2015.

Basarir, H., Tutluoglu, L., and Karpuz, C., Penetration Rate Prediction for Diamond Bit Drilling by Adaptive Neuro-fuzzy Inference System and Multiple Regressions, Engineering Geology, Vol. 173, p. 1-9, 2014.

Bilgesu, H., Tetrick, L., Altmis, U., Mohaghegh, S., and Ameri, S., A New Approach for the Prediction of Rate of Penetration (ROP) Values, Paper presented at the SPE Eastern Regional Meeting, 1997.

Bodaghi, A., Ansari, H. R., and Gholami, M., Optimized Support Vector Regression for Drilling Rate of Penetration Estimation, Open Geosciences, Vol. 7, No. 1, p. 870-879, 2015.

Bourgoyne, A. T., Millheim, K. K., Chenevert, M. E., and Young, F. S., Applied Drilling Engineering (Vol. 2): Society of Petroleum Engineers Richardson, TX, 1991.

Bourgoyne Jr, A. T., and Young Jr., F., A Multiple Regression Approach to Optimal Drilling and Abnormal Pressure Detection, Society of Petroleum Engineers Journal, Vol. 14, No. 04, p. 371-384, 1974.

Eren, T., Real-Time Optimization of Drilling Parameters during Drilling Operations, Middle East Technical University, 2010.

Eren, T., Real-time Optimization of Drilling Parameters During Drilling Operations (Master Thesis), School of Natural and Applied Science of Middle East Technical University, Turkey, 2010.

Granville, V., Krivánek, M., and Rasson, J.P., Simulated Annealing: A Proof of Convergence, IEEE Transactions on Pattern Analysis and Machine Intelligence, Vol. 16, No. 6, p. 652-656, 1994.

Hareland, G. and Rampersad, P., Drag-bit Model Including Wear, Paper presented at the SPE Latin America/Caribbean Petroleum Engineering Conference, 1994.

Hegde, C., Wallace, S., and Gray, K., Using Trees, Bagging, and Random Forests to Predict Rate of Penetration During Drilling, Paper presented at the SPE Middle East Intelligent Oil and Gas Conference and Exhibition, 2015.

Jang, J.S., ANFIS: Adaptive-network-based Fuzzy Inference System, IEEE Transactions on Systems, Man, and Cybernetics, Vol. 23, No. 3, p. 665-685, 1993.

Jiang, W. and Samuel, R., Optimization of Rate of Penetration in a Convoluted Drilling Framework Using Ant Colony Optimization, Paper presented at the IADC/SPE Drilling Conference and Exhibition, 2016.

Kahraman, S., Estimating the Penetration Rate in Diamond Drilling in Laboratory Works Using the Regression and Artificial Neural Network Analysis, Neural Processing Letters, Vol. 43, No. 2, p. 523-535, 2016.

Khandelwal, M. and Armaghani, D. J., Prediction of Drillability of Rocks with Strength Properties Using a Hybrid GA-ANN Technique, Geotechnical and Geological Engineering, Vol. 34, No. 2, p. 605-620, 2016.

Khosravanian, R., Sabah, M., Wood, D. A., and Shahryari, A., Weight on Drill Bit Prediction Models: Sugeno-type and Mamdani-type Fuzzy Inference Systems Compared, Journal of Natural Gas Science and Engineering, Vol. 36, p. 280-297, 2016.

Kirkpatrick, S., Gelatt, C. D., and Vecchi, M. P., Optimization by Simulated Annealing, Science, Vol. 220, No. 4598, p. 671-680, 1983.

Liu, Z., Marland, C. N., Li, D., and Samuel, R., An Analytical Model Coupled with Data Analytics to Estimate PDC Bit Wear, Paper presented at the SPE Latin America and Caribbean Petroleum Engineering Conference, 2014.

Mathur, N., Glesk, I., and Buis, A., Comparison of Adaptive Neuro-fuzzy Inference System (ANFIS) and Gaussian Processes for Machine Learning (GPML) Algorithms for the Prediction of Skin Temperature in Lower Limb Prostheses, Medical Engineering and Physics, Vol. 38, No. 10, p. 1083-1089, 2016.

Metropolis, N., Rosenbluth, A. W., Rosenbluth, M. N., Teller, A. H., and Teller, E., Equation of State Calculations by Fast Computing Machines, The Journal of Chemical Physics, Vol. 21, No. 6, p. 1087-1092, 1953.

Monazami, M., Hashemi, A., and Shahbazian, M., Drilling Rate of Penetration Prediction Using Artificial Neural Network: A Case Study of One of Iranian Southern Oil Fields, Electronic Scientific Journal Oil and Gas Business, Vol. 6, No. 6, p. 21-31, 2012.

Moraveji, M. K. and Naderi, M., Drilling Rate of Penetration Prediction and Optimization Using Response Surface Methodology and Bat Algorithm, Journal of Natural Gas Science and Engineering, Vol. 31, p. 829-841, 2016.

Nascimento, A., Tamas Kutas, D., Elmgerbi, A., Thonhauser, G., and Hugo Mathias, M., Mathematical Modeling Applied to Drilling Engineering: An Application of Bourgoyne and Young ROP Model to a Presalt Case Study, Mathematical Problems in Engineering, 2015.

Nedjah, N. and de Macedo Mourelle, L., Fuzzy Systems Engineering: Theory and Practice (Vol. 181): Springer Science and Business Media, 2005.

Rabiei, A., Sayyad, H., Riazi, M., and Hashemi, A., Determination of Dew Point Pressure in Gas Condensate Reservoirs Based on a Hybrid Neural Genetic Algorithm, Fluid Phase Equilibria, Vol. 387, No. 38-49, 2015.

Rahimzadeh, H., Mostofi, M., and Hashemi, A., A New Method for Determining Bourgoyne and Young Penetration Rate Model Constants, Petroleum Science and Technology, Vol. 29, No. 9, p. 886-897, 2011.

Rahimzadeh, H., Mostofi, M., Hashemi, A., and Salahshoor, K., Comparison of the Penetration Rate Models Using Field Data for One of the Gas Fields in Persian Gulf Area, Paper presented at the International Oil and Gas Conference and Exhibition in China, 2010.

Shadizadeh, S., Karimi, F., and Zoveidavianpoor, M., Drilling Stuck Pipe Prediction in Iranian Oil Fields: An Artificial Neural Network Approach, Iran J. Chem. Eng., Vol. 7, No. 4, p. 29-41, 2010.

Shi, X., Liu, G., Gong, X., Zhang, J., Wang, J., and Zhang, H., An Efficient Approach for Real-time Prediction of Rate of Penetration in Offshore Drilling, Mathematical Problems in Engineering, 2016.

Shi, X., Meng, Y., Li, G., Li, J., Tao, Z., and Wei, S., Confined Compressive Strength Model of Rock for Drilling Optimization, Petroleum, Vol. 1, No. 1, p. 40-45, 2015.

Sugeno, M. and Kang, G., Structure Identification of Fuzzy Model, Fuzzy Sets and Systems, Vol. 28, No. 1, p. 15-33, 1988.

Wang, Y., Bu, G., Wang, Y., Zhao, T., Zhang, Z., and Zhu, Z., Application of a Simulated Annealing Algorithm to Design and Optimize a Pressure-swing Distillation Process, Computers and Chemical Engineering, Vol. 95, p. 97-107, 2016.

Yi, P., Kumar, A., and Samuel, R., Real-time Rate of Penetration Optimization Using the Shuffled Frog Leaping Algorithm (SFLA), Paper presented at the SPE Intelligent Energy Conference and Exhibition, 2014.

Zoveidavianpoor, M., Samsuri, A., and Shadizadeh, S. R., Adaptive Neuro Fuzzy Inference System for Compressional Wave Velocity Prediction in a Carbonate Reservoir, Journal of Applied Geophysics, Vol. 89, p. 96-107, 2013.

Zoveidavianpoor, M., Samsuri, A., and Shadizadeh, S. R., Prediction of Compressional Wave Velocity by an Artificial Neural Network Using some Conventional Well Logs in a Carbonate Reservoir, Journal of Geophysics and Engineering, Vol. 10, No. 4, p. 045014, 2013.